On the Use of the Matrix-Pencil Method to Correlate Measurements at Different Test Sites

Benoît Fourestié, Zwi Altman, *Senior Member, IEEE*, Joe Wiart, *Member, IEEE*, and Alain Azoulay

***Abstract*—A new method for systematic correlation of measurements in semi-anechoic and anechoic chambers is presented. A signal measured in a semi-anechoic chamber is first processed using the matrix-pencil method which is applied sequentially on small frequency intervals. On each interval the measured signal is decomposed into its propagating wave components. The component corresponding to the wave reflected from the ground is identified and removed to fully retrieve the signal measured in an anechoic chamber. Three examples using log-periodic and Vivaldi antennas in different anechoic and semi-anechoic chambers for varying frequency ranges illustrate the method. The proposed decomposition algorithm can be utilized to characterize measurement test site imperfections.**

***Index Terms*— Anechoic chamber (electromagnetic), antenna measurements, matrix-pencil method, measurements, (semi-)anechoic chamber, test site.**

I. Introduction

MEASUREMENT test sites fall into two main categories: sites which are ideally free of reflections such as anechoic chambers and sites with reflecting ground such as semi-anechoic chambers and open-area test sites (OATS). The nature of electromagnetic wave propagation differs in these different test sites due to varying reflections from the ground or absorbing materials, if present, and contingent resonance phenomena. For a given experimental setup of a radiating source and a receiving antenna, measured results are likely to vary for each different test site. Therefore, standards of measurements are specific to each type of site [1]–[3].

A model based on the geometrical-optics approximation with the assumption of a perfectly reflecting ground plane has been proposed to correlate measurements performed in anechoic and semi-anechoic chambers. However, such a simplified model has a limited domain of validity and often leads to correlation with poor accuracy [4].

To make possible measurement correlation, it is necessary to characterize test site imperfections. Site characterization can be carried out either in frequency or in time domain [5]. In the frequency domain, measurements of normalized site attenuation (NSA) [6] necessitate an *a priori* knowledge of certain antenna parameters such as the antenna factor in a given direction. The frequency-domain approach for anechoic chambers described in [7] involves measuring the interference pattern by moving one of the antennas and carefully scanning the quiet zones. Time-domain approaches are comparatively more accurate, but they require complicated equipment such as pulse generators and fast sampling oscilloscopes [8], [9].

The aim of this work is to put forward a new method for systematic retrieval of results obtained in an anechoic chamber from results measured in a semi-anechoic chamber using the matrix-pencil method [10]. It is assumed that the measurements are available in both amplitude and phase. The following strategy is proposed to correlate measurement results. First, the measured signal is decomposed into a small number of complex exponential functions. Then, the exponential functions are processed to identify the terms corresponding to the different propagating components, viz., the direct and the reflected wave components. Once identified, the term corresponding to the reflected component is removed to retrieve the signal obtained in an anechoic chamber.

The matrix-pencil method or its previous version, the generalized pencil of function method (GPOF) method [11], are both robust and accurate techniques for decomposing signals into a sum of complex exponential functions. They have been successfully applied to various problems in electromagnetics such as the extrapolation of time signatures in the finite-difference time-domain (FDTD) method [12], the representation of induced currents over large and smooth scatterers [13] and the solution for a class of large-body scattering problems [14]. Every continuous function with finite support can be described as a series of complex exponential functions. The use of the matrix-pencil method is of particular interest when the signal is composed of the sum of only a few complex exponentials. In many cases, other types of functions, such as oscillating functions with algebraic attenuation, can be accurately decomposed into a sum of a few complex exponentials provided that the interval in which they are considered is relatively narrow.

The paper is organized as follows. In Section II, the correlation technique based on the matrix-pencil method is described. Three examples of the proposed technique applied for different measurement configurations are presented in Section III, followed by a discussion and concluding remarks in Section IV.

II. Analysis

Consider a system consisting of two antennas facing each other in a semi-anechoic chamber (Fig. 1). The transmission coefficient of the system, $S_{21}^{\text{semi}}(f)$ is measured as a function of frequency f. $S_{21}^{\text{semi}}(f)$ includes both the contributions of the direct propagating component and the component reflected

Manuscript received April 6, 1998; revised February 15, 1999.

B. Fourestié, Z. Altman, and J. Wiart are with the Centre National d'Etude des Télécommunications, 92794 Issy Moulineaux Cedex 9, France.

A. Azoulay is with Télédiffusion De France, 78897 Saint Quentin, France.

Publisher Item Identifier S 0018-926X(99)09384-9.

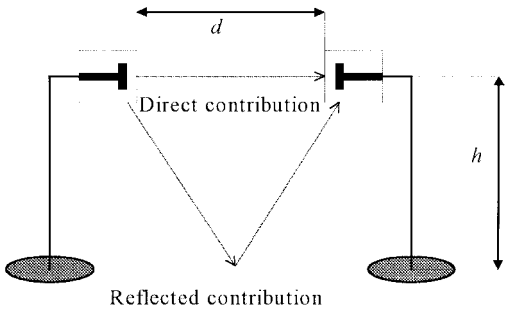

Fig. 1. Antenna setup for transmission coefficient measurements.

from the ground. Ideal absorbers are assumed at the frequency range under consideration.

With a view to physically identify the propagating components of the measured signal, we undertake the decomposition of $S_{21}^{\text{semi}}(f)$ into a sum of complex exponentials

$$S_{21}^{\text{semi}}(f) = \sum_{i=1}^{M} c_i e^{\gamma_i f} \tag{1}$$

where γ_i's are complex numbers of the form $\gamma_i = \alpha_i + j\beta_i$. α_i's are damping factors required to represent $S_{21}^{\text{semi}}(f)$ in terms of complex exponential functions. They take into account the attenuation due to propagation, reflections, and antenna factors. β_i has the dimension of radian $\times$ second and is related to the propagation time of the ith component between the two antennas. The product $\beta_i f$ is related to the phase accumulation of the direct component ($i = 1$) between the two antennas

$$\varphi_1 = \beta_1 f = \frac{2\pi d}{c} f \bmod(2\pi) = 2\pi t_1 f \bmod(2\pi) \tag{2}$$

where t_1 is the time needed for the direct propagating component to travel a distance d between the two antennas at the velocity of light in free-space c. When considering the reflected component, one should add to the phase lag corresponding to the propagation delay an additional phase taking into account the reflection on the ground.

The coefficients c_i and γ_i can be derived by sampling $S_{21}^{\text{semi}}(f)$ uniformly at frequencies f_k, $f_k = (k-1)\Delta f$ and applying the matrix-pencil method to the sampled signal

$$S_{21}^{\text{semi}}(k) = \sum_{i=1}^{M} c_i e^{\gamma_i (k-1)\Delta f}. \tag{3}$$

In the present work, the entire frequency range has been divided into subintervals with a width corresponding to a cycle of the beat frequency of the direct component and the component reflected at the ground. Following the matrix-pencil procedure [10], [11], measurement data are laid out into a complex matrix $[Y]$. To estimate the number M of poles, i.e., the number of complex exponentials necessary to accurately decompose the signal over each subinterval, a singular value decomposition (SVD) is performed on $[Y]$. For noiseless data, the number of poles can be estimated from the number of nonzero singular values. For noisy data, such as considered here, singular values which are deemed to be below noise level are discarded. We therefore apply a cutoff criterion in the SVD which is determined by a threshold ε

$$\frac{\sigma_i}{\sigma_{\max}} \leq \varepsilon \tag{4}$$

where σ_i is the singular value under consideration and $\sigma_{\max}$ the highest singular value corresponding to the direct propagating wave. The value for ε, which defines the upper limit for the error introduced by the SVD reconstruction, is chosen as one over the signal-to-noise ratio (SNR). SNR values of 25–30 dB can be easily achieved with the experimental setup, and a value of 30 dB has been chosen throughout this work.

Respecting the above cutoff criterion, $S_{21}^{\text{semi}}(f)$ can be accurately described on each subinterval using three complex exponentials: the direct and the reflected propagating components and a third component that can be viewed as a corrective term related to the antenna factors. From the list of complex exponential functions generated by the matrix-pencil routine, we find those related to the propagating components. The identification of the two propagating components can be performed assuming two hypotheses.

1) The phase of the direct and reflected components are continuous with frequency, i.e., β_i's are continuous for $i = 1, 2$.
2) The amplitude of the direct component is greater than that of the reflected one. The contribution of the third exponential is small compared to the two others.

Once the three exponentials are successfully identified, the contribution coming from the ground can be removed. We thus reconstruct the signal $S_{21}^{\text{anec}}(f)$ that would be measured using the same system in a fully anechoic chamber.

The presence of noise in the measured data can make the identification of the exponentials a difficult task and is error prone when reconstructing the signal on each subinterval. To reduce the influence of noise we propose the following averaging procedure. Denote by I_i the subinterval $[S_{21}^{\text{semi}}(i);\ S_{21}^{\text{semi}}(L+i-1)]$, where L is the number of samples in each subinterval. The decomposition (3) is applied over the subintervals I_1 to I_{N-L+1}, where N is the total number of samples. Each sample k belongs to p_k different subintervals

$$p_k = \begin{cases} k; & k = 1, \cdots, L \\ L; & k = L+1, \cdots, N-L \\ N+1-k; & k = N-L+1, \cdots, N. \end{cases} \tag{5}$$

Denote by the subscript s the interval number to which the kth sample belongs and by $S_{21,\,s}^{\text{recon}}(k)$ the computed value of $S_{21}^{\text{recon}}(k)$ in subinterval s. We can write the reconstructed signal as follows:

$$S_{21}^{\text{recon}}(k) = \frac{1}{p_k} \sum_{s=1}^{p_k} S_{21,\,s}^{\text{recon}}(k). \tag{6}$$

This averaging, which can be considered as a lowpass filtering increases the accuracy of the reconstruction. Moreover, it allows one to fully exploit the continuity of the phase during the complex exponential identification process.

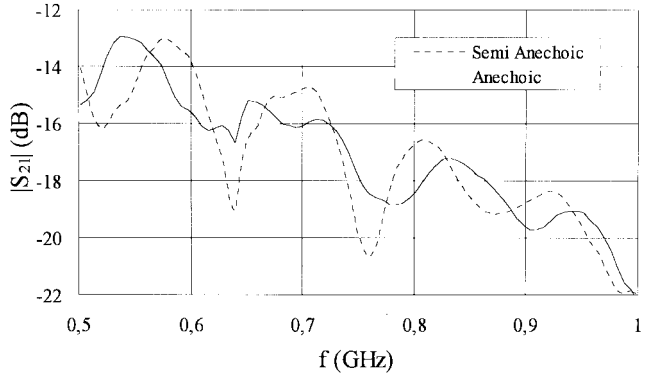

Fig. 2. Comparison of the signal measured in a semi-anechoic chamber $S_{21}^{\text{semi}}(f)$ with the signal measured in a fully anechoic chamber $S_{21}^{\text{anec}}(f)$ for log-periodic antennas separated by a distance of 1 m in horizontal polarization.

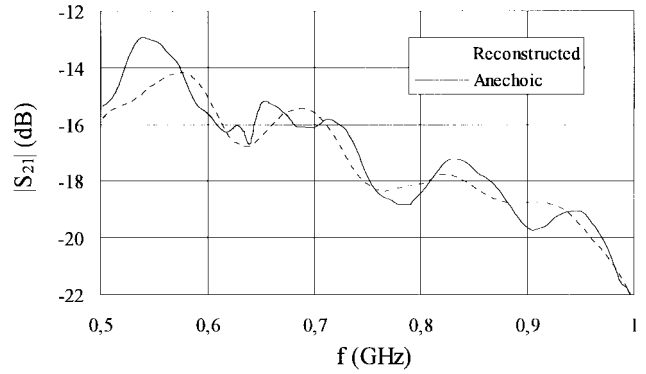

Fig. 3. Comparison of the reconstructed signal $S_{21}^{\text{recon}}(f)$ with the signal measured in a fully anechoic chamber $S_{21}^{\text{anec}}(f)$ for log-periodic antennas separated by a distance of 1 m in horizontal polarization.

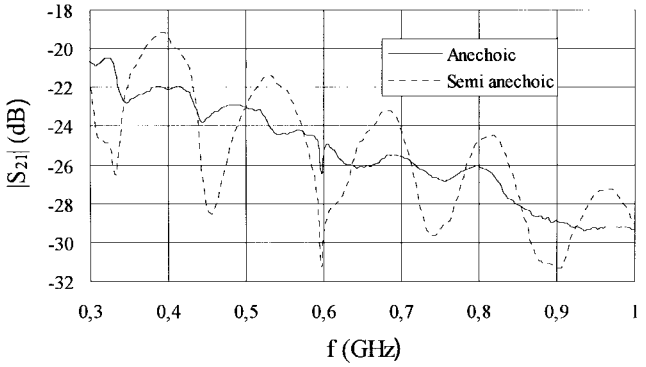

Fig. 4. Comparison of signal measured in a semi-anechoic chamber $S_{21}^{\text{semi}}(f)$ with the signal measured in a fully anechoic chamber $S_{21}^{\text{anec}}(f)$ for log-periodic antennas separated by a distance of 3 m in horizontal polarization.

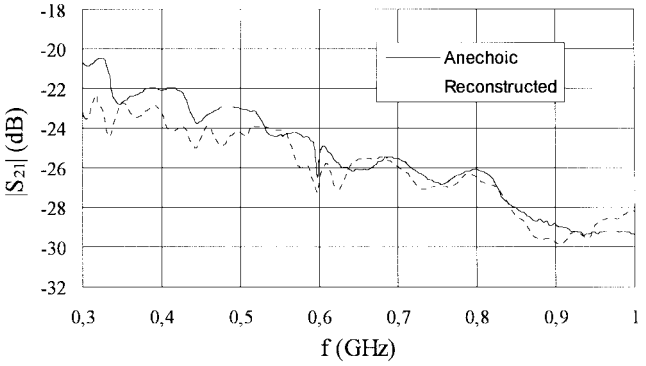

Fig. 5. Comparison of the reconstructed signal $S_{21}^{\text{recon}}(f)$ with the signal measured in a fully anechoic chamber $S_{21}^{\text{anec}}(f)$ for log-periodic antennas separated by a distance of 3 m in horizontal polarization.

III. Results

The transmission parameters $S_{21}^{\text{semi}}(f)$ for different types of antennas were measured using the Network Analyzer Wiltron 360 B. The Network Analyzer was calibrated to remove the influence of the cables and connecting devices. The measured signal was sampled uniformly and the matrix pencil can be applied directly to the measured samples without any preprocessing.

The reconstructed signal $S_{21}^{\text{recon}}(f)$ derived as explained above was compared to measured results of $S_{21}^{\text{anec}}(f)$ obtained using the same measuring system and antenna configuration in a fully anechoic chamber. The fully anechoic chamber was obtained by adding absorbing material on the ground. $S_{21}^{\text{anec}}(f)$ was taken as a reference to validate the proposed method.

In the first example, measurements were carried out in a $3.05 \times 4.20 \times 2.85$ m^3 semi-anechoic chamber using two log-periodic dipole array antennas with a nominal frequency bandwidth of 200–1000 MHz in horizontal polarization, facing each other at a distance of 1 m. The frequency range considered was 500–1000 MHz ensuring good performance of the absorbing materials and the frequency sampling step was $\Delta f = 6$ MHz. The two antennas were situated 1 m above the ground. Measured results for $S_{21}^{\text{semi}}(f)$ and $S_{21}^{\text{anec}}(f)$ are shown in Fig. 2 and the comparison between the reconstructed signal $S_{21}^{\text{recon}}(f)$ and $S_{21}^{\text{anec}}(f)$ is presented in Fig. 3. The difference between $S_{21}^{\text{recon}}(f)$ and $S_{21}^{\text{anec}}(f)$ does not exceed 2.3 dB over the whole frequency range, with an average difference of only 0.4 dB and a standard deviation of 0.59 dB. For frequencies above 550 MHz, the difference remains below 1.8 dB.

Next, we consider measurements performed in a $11.2 \times 7.2 \times 7.6$ m^3 semi-anechoic chamber. Two log-periodic antennas with a nominal frequency bandwidth of 100–1000 MHz were set up in horizontal polarization, 2 m above the ground, and 3 m apart. Measurements of $S_{21}^{\text{semi}}(f)$ and $S_{21}^{\text{anec}}(f)$ were carried out in the frequency range of 300–1000 MHz with a sampling step of $\Delta f = 3.6$ MHz (Fig. 4). The difference between $S_{21}^{\text{anec}}(f)$ and $S_{21}^{\text{recon}}(f)$ over the entire frequency range is less than 3.5 dB and is equal to 0.6 dB on average with a standard deviation of 0.84 dB (Fig. 5). When considering the frequency range 350–1000 MHz, the difference is less than 2.3 dB.

In the third example, measurements of $S_{21}^{\text{semi}}(f)$ and $S_{21}^{\text{anec}}(f)$ were performed using two broad-band Vivaldi antennas in the frequency range of 1–11 GHz (Fig. 6). The antennas were set up in vertical polarization 1 m apart and 1 m above the ground. Frequency samples were measured at a step of $\Delta f = 60$ MHz over the whole frequency range. The reconstructed signal $S_{21}^{\text{recon}}(f)$ is remarkably accurate. It differs from $S_{21}^{\text{anec}}(f)$ by less than 1.8 dB, by 0.3 on average with a standard deviation of 0.42 dB (Fig. 7). At frequencies above 2 GHz, the difference is below 1.2 dB.

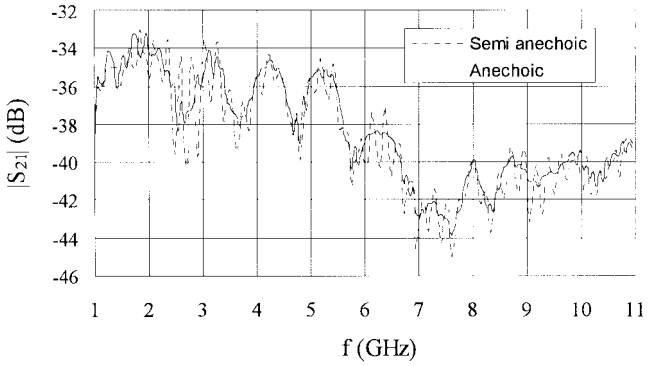

Fig. 6. Comparison of the signal measured in a semi-anechoic chamber $S_{21}^{\text{semi}}(f)$ with the signal measured in a fully anechoic chamber $S_{21}^{\text{anec}}(f)$ for Vivaldi antennas separated by a distance of 1 m in vertical polarization.

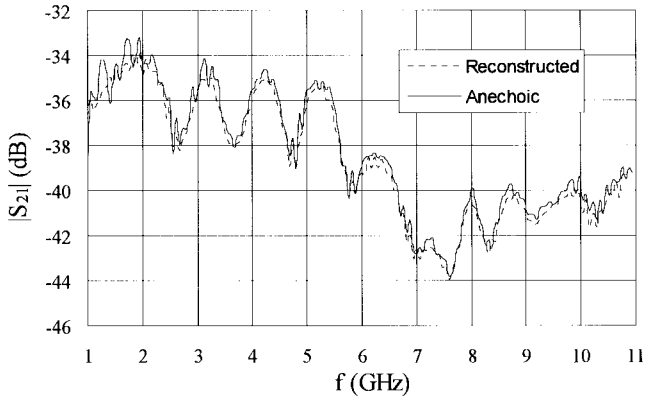

Fig. 7. Comparison of the reconstructed signal $S_{21}^{\text{recon}}(f)$ with the signal measured in a fully anechoic chamber $S_{21}^{\text{anec}}(f)$ for Vivaldi antennas separated by a distance of 1 m in vertical polarization.

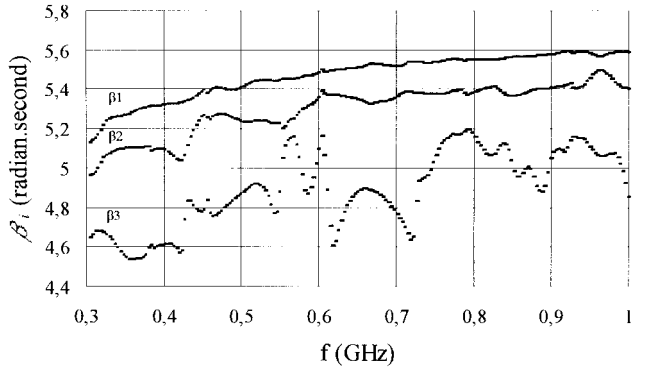

Fig. 8 Evolution of β_i with frequency for log-periodic antennas in horizontal polarization 3 m apart.

We terminate this section by making some remarks on the frequency behavior of the β_i's. Consider first the example of the log-periodic dipole array. At a given frequency, the radiating part of the antenna (called the active region) is located around the elements of length close to that of a tuned dipole at the considered frequency [17], [18]. The active region and its associated phase center move with frequency along the array and so the distance separating the phase centers of the two log-periodic antennas is a function of frequency. From (2) we can see that β_1 is also a function of frequency, and in a similar manner we can extend this result to β_2. The frequency dependence of the β_i's for the log-periodic antennas is shown in Fig. 8.

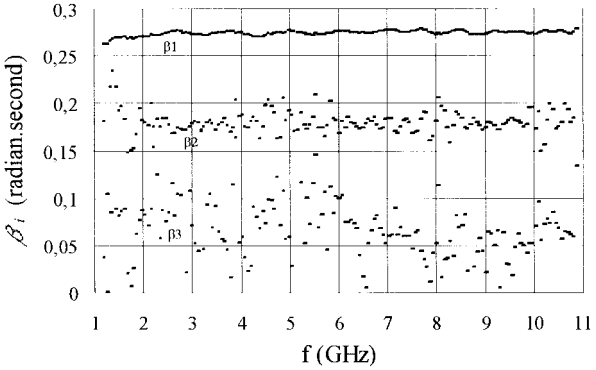

Fig. 9. Evolution of β_i with frequency for Vivaldi antennas in vertical polarization 1 m apart.

In the matrix-pencil method the β_i's, $i = 1, 2, 3$, are assumed constant over each frequency subinterval. For systems in which β_i's are functions of frequency, this assumption entails small errors in the reconstruction of the signal $S_{21}^{\text{recon}}(f)$. However, this error is minimized by using the aforementioned averaging procedure.

Processed measurement results using the Vivaldi antennas show that β_1 of the direct propagating component does not show any notable frequency dependence over the whole frequency range (Fig. 9). This result brings us to the interesting conclusion that the location of the phase center of the Vivaldi antenna remains practically unchanged with frequency.

IV. Conclusion

A method for systematic retrieval of measurements in a fully anechoic chambers from measurements in a semi-anechoic chamber has been developed in this paper. This method shows its usefulness in the case of antenna testing or measurement site validation. It is based on a decomposition of the measured signal into its propagating components in the form of complex exponential functions over narrow frequency intervals using the matrix-pencil method. It has been shown that the component reflected at the ground can be identified and removed from the measured data. Using the presented correlation technique in three different examples for varying frequency ranges, antennas, and configurations, the results of measurements performed in fully anechoic chambers have been retrieved from those performed in semi-anechoic chambers.

The proposed method has several attractive features: no *a priori* knowledge of the system such as antenna factors or system configuration is needed. The algorithm requires very little computational resources. Unlike techniques based on Fourier transform of data sampled in the frequency domain, the proposed method is independent of the frequency bandwidth under consideration and narrow-band signals can be handled adequately. Furthermore, its requirements in terms of frequency sampling step remain low.

A straightforward extension of the method can be envisaged for lower frequencies. The presence of several reflections in the test site should be handled by decomposing the signal using more exponential terms. First encouraging results in the frequency range of 50–300 MHz have been obtained using five to six complex exponentials in the decomposition.

The correlation method could then be used for characterizing measurement site imperfections such as poor performance of absorbing materials, parasitic reflections, or coupling effects.

REFERENCES

[1] "Specification for radio disturbance and immunity measuring apparatus and methods," Int. Special Committee Radio Interference, CISPR, 16-1, 1993.

[2] "American national standard: Methods of measurements of radio noise emissions from low voltage electrical and electronic equipment in the range of 10 kHz to 1 GHz," ANSI C63.4, 1988.

[3] "American national standard for calibration of antennas used for radiated emission measurements in electromagnetic interference (EMI) control," Amer. Nat. Standard Inst., ANSI C63.5, 1988.

[4] W. S. Bennett, "Comments on 'Calculation of site attenuation from antenna factors'," *IEEE Trans. Electromagn. Compat.*, vol. EMC-25, pp. 121–124, May 1983.

[5] G. E. Evans, *Antenna Measurement Techniques.* Norwood, MA: Artech House, 1990, pp. 85–99

[6] A. Sugiura, "Formulation of normalized site attenuation in terms of antenna impedances," *IEEE Trans. Electromagn. Compat.*, vol. 32, pp. 257–263, Nov. 1990.

[7] J. Appel-Hansen, "Reflectivity level of radio anechoic chambers," *IEEE Trans. Antennas Propagat.*, vol. AP-21, pp. 490–498, 1973.

[8] E. N. Clouston, P. A. Langsford, and S. Evans, "Measurement of anechoic chamber reflections by time-domain techniques," *Proc. IEEE*, vol. 135, pt. H, pp. 93–97, Apr. 1988.

[9] S. Tofani, A. Ondrejka, and M. Kanda, "A time-domain method for characterizing the reflection coefficient of absorbing materials from 30–1000 MHz," *IEEE Trans. Electromagn. Compat.*, vol. 33, pp. 234–240, Aug. 1991.

[10] R. S. Adve, T. K. Sarkar, O. M. C. Pereira-Filho, and S. M. Rao, "Extrapolation of time-domain responses from three-dimensional conducting objects utilizing the matrix-pencil technique," *IEEE Trans. Antennas Propagat.*, vol. 45, pp. 147–155, Jan. 1997.

[11] Y. Hua and T. K. Sarkar, "Generalized pencil-of-function method for extracting poles of an EM system from its transient response," *IEEE Trans. Antennas Propagat.*, vol. 37, pp. 229–234, Feb. 1989.

[12] W. L. Ko, M. I. Aksun, and R. Mittra, "A generalized eigenvalue method for FDTD analysis," *Microwave Opt. Tech. Lett.*, vol. 6, pp. 552–554, July 1993.

[13] Z. Altman, R. Mittra, O. Hashimoto and E. Michelssen, "Efficient representation of induced currents on large scatterers using the generalized pencil of function method," *IEEE Trans. Antennas Propagat.*, vol. 44, pp. 51–57, Jan. 1996.

[14] J. C. Goswami and R. Mittra, "On the solution of a class of large-body scattering problems via the extrapolation of FDTD solutions," *J. Electromagn. Waves Applicat.*, Dec. 1997.

[15] G. H. Golub and C. F. Van Loan, *Matrix Computations.* Baltimore, MD: Johns Hopkins Univ. Press, 1989.

[16] T. K. Sarkar and O. M. C. Pereira-Filho, "Using the matrix-pencil method to estimate the parameters of a sum of complex exponentials," *IEEE Antennas Propagat. Mag.*, vol. 37, pp. 48–55, Feb. 1995.

[17] R. Mittra, "Log-periodic antennas," in *Antenna Theory*, R. E. Collin and F. J. Zucker, Eds. New York: McGraw-Hill, 1969, ch. 22, pt. 2, pp. 378–380.

[18] C. A. Balanis, *Antenna Theory: Analysis and Design.* New York: Wiley, 1982, pp. 427–439.

Benoît Fourestié was born in Paris, France, in 1975. He received the telecommunication engineering degree from the Institut National des Télécommunications, Evry, France, in 1997, and the D.E.A. degree in digital telecommunication systems from the Ecole Nationale Supérieure des Télécommunications, Paris, France, in 1997. He is currently working toward the Ph.D. degree in electrical engineering at the CNET-National Center of Telecommunication Studies of France Telecom, Issy les Moulineaux, France.

His research interests include antenna measurements, near-field techniques, electromagnetic compatibility, statistics, and signal processing.

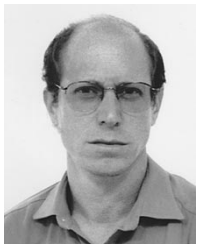

Zwi Altman (S'88–M'90–SM'98) received the B.Sc. and M.Sc. degrees in electrical engineering from the Technion-Israel Institute of Technology, Haifa, in 1986 and 1989, respectively, and the Ph.D. degree in electronics from the Institut National Polytechnique de Toulouse, France, in 1994.

He was a "Lauréat de la Bourse LAVOISIER" of the French Foreign Ministry in 1994 and from 1994 to 1996 he was a Postdoctoral Research Fellow at the Electromagnetic Communication Laboratory, Electrical Engineering Department, University of Illinois, Urbana-Champaign. In 1996 he joined the CNET-National Center of Telecommunication Studies of France Telecom, Issy les Moulineaux, France. His research interests include electromagnetic compatibility, bioelectromagnetics, antenna measurements, computational electromagnetics, and signal processing.

Dr. Altman is currently an Associate Editor for the IEEE TRANSACTIONS ON ELECTROMAGNETIC COMPATIBILITY.

Joe Wiart (M'96) received the Engineer degree from the Ecole Nationale Supérieure des Télécommunications, Paris, France, in 1992, and the Ph.D. degree in physics from the ENST and P&M Curie University, Paris, France, in 1995.

He joined the CNET, the research center of France Telecom, issy les Moulineaux, in 1992, and spent three years working on propagation in a microcellular environment. Since 1994 he has been working on the interaction of radiowaves with the human body and on medical electronic devices. He is currently the head of a group dealing with these questions in CNET. His research interests include electromagnetic compatibility, bioelectromagnetics, antenna measurements, computational electromagnetics, and signal processing.

Dr. Wiart is Vice Chairman of the COST 244b, Chairman of the CENELEC Working Group in charge of mobile and base station standards and Vice Chairman of the URSI French Commission K. He has been a senior member of the SEE since 1998.

Alain Azoulay received the Engineer degree from Ecole Supérieure d'Electricité, Gif sur Yvette, France, in 1970.

After having worked at Thomson CSF on microwave relays, he joined CNET, the research center of France Telecom, Issy les Moulineaux, in 1974, where he has been involved in tropospheric propagation studies, electromagnetic compatibility (EMC), and mobile communications and was head of the Radio EMC and Mobile Department until 1997. In 1998, he moved to Télédiffusion de France, the subsidiary of France Telecom for broadcasting, where he is currently Head of the Radio and EMC Measurement Department.

Dr. Azoulay has been Chairman of ITU-R Task Group 1/3 on spurious emission of transmitters until 1997. He is currently a member of the European Broadcasting Union and member of the CISPR (International Committee on Radio Interference).